Measurement of the Reaction $\pi^- p \to \pi^0 n$ at Large Momentum Transfers*

W. S. Brockett, G. T. Corlew, W. R. Frisken, T. L. Jenkins, A. R. Kirby, C. R. Sullivan, and J. A. Todoroff†
Case Western Reserve University, Cleveland, Ohio 44106

and

W. B. Richards
Oberlin College, Oberlin, Ohio 44074
(Received 10 November 1970)

We present results of an experiment to measure the differential cross section of the reaction $\pi^- p \to \pi^0 n$ between the forward and backward peaks. The measurements were made at incident π^- momenta of 3.67 and 4.83 GeV/c. The t range $1.7 \leq |t| \leq 4.9$ (GeV/c)^2 was covered at the lower momentum and $1.8 \leq |t| \leq 7$ (GeV/c)^2 at the higher momentum. At the lower momentum the cross section is essentially constant between $|t| = 2.4$ and 4.8 (GeV/c)^2 while at the higher momentum the angular distribution exhibits a broad minimum centered at $|t| = 4.4$ (GeV/c)^2.

We report a measurement of the differential cross section for charge-exchange scattering $\pi^- p \to \pi^0 n$ in the region of high momentum transfer. Incident pions of momenta 3.67 and 4.83 GeV/c were obtained in the 17° beam of the zero-gradient synchrotron (ZGS) at Argonne National Laboratory. Previous experiments[1-3] had already measured the forward and backward peaks and the present experiment was designed to be sensitive in the high-momentum-transfer region in between. Regge-pole models[4] have predicted a dip in the cross section at $t = -2.5$ (GeV/c)^2, and recent data[5] in the elastic channels of the $\pi^- p$ and $\pi^+ p$ interactions show a pronounced dip in the region of $-t = 2.8$-3.0 (GeV/c)^2.

The apparatus is shown in Fig. 1. The π^- beam was momentum analyzed to ±0.75% and focused on a 10-cm-long liquid-hydrogen target. The beam-defining counters consisted of a quadruple scintillator telescope, B_1 through B_4, together with an array of beam-halo veto counters A_{17}-A_{20}. The threshold Cherenkov counter between B_1 and B_2 was used to veto higher-mass particles. The output of this telescope was vetoed by any beam particle which preceded it by less than 1 μsec. The final result was a signal, designated B, which typically ran at 10^5/sec. Thin-plate spark chambers, S_3 and S_4, in the beam located the trajectory of the incident particle.

The basic left-right symmetry of the apparatus

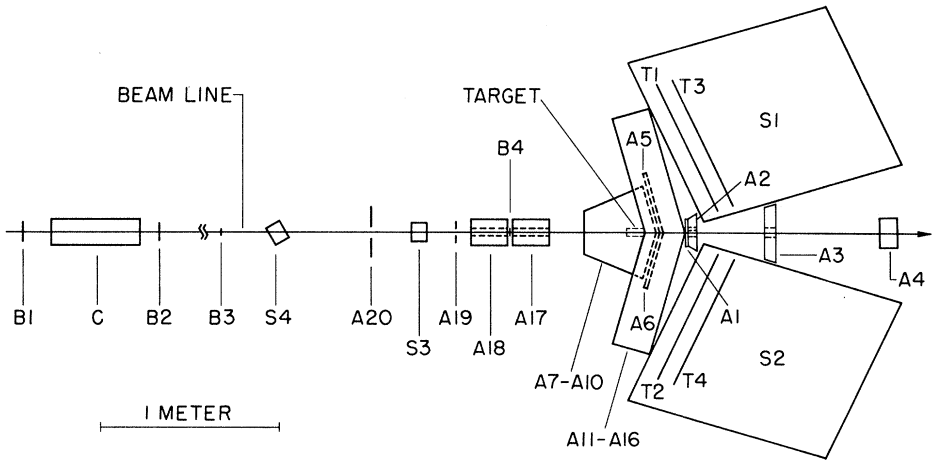

FIG. 1. Plan view of the apparatus. The beam telescope consisted of B_1 through B_4. C is a gas Cherenkov counter. All counters designated A were used as vetos. A_1, A_5, A_6, A_{19}, and A_{20} were simple scintillation counters; all other veto counters consisted of lead-scintillator sandwiches. The counters A_7 through A_{10} formed an enclosure around the target and in turn were surrounded by a rectangular structure consisting of counters A_{11} through A_{16}. Counters T_1 through T_4 were scintillation counters embedded in the chamber arrays (S_1 and S_2) which produced the "T" signal. S_3 and S_4 were thin-plate spark chambers.

arises because the momentum-transfer region under investigation is centered around the case where the π^0 and neutron have equal angles in the lab system. The arrays, S_1 and S_2, of alternating converter plates and spark chambers on either side of the beam were designed to detect either photons (from $\pi^0 \to 2\gamma$) or neutrons. Each of the first five converter plates consisted of 3.75 g/cm^2 of lead, a total of 2.25 photon conversion lengths. The remaining twenty plates were each 15 g/cm^2 of lead, a total of 1.5 interaction mean free paths for neutrons in this energy range. Since the neutron conversion length is about 25 times the photon conversion length, a typical event would have two γ showers near the front, for example, of the array S_1 with a neutron conversion deep in the array S_2. The spark chambers were two-gap modules having a sensitive area 36 in. square.

The target was surrounded by an arrangement of veto counters which (a) ensured that no charged particle entered the sensitive regions S_1 or S_2, and (b) strongly suppressed events in which strongly or electromagnetically interacting particles entered the remaining solid angle. The veto counters providing this latter function consisted of a group of counters directly downstream of the target (A_1-A_4), a group of shower counters arranged in a boxlike structure close to and surrounding the target (A_7-A_{10}), and a third group of shower counters (A_{11}-A_{16}) arranged in a rectangular structure midway between the target and the chamber arrays. This last group served to define the solid angle subtended by the neutral-particle veto system more cleanly than could have been done by the A_7-A_{10} group alone, owing to the nonzero target length. This entire system delivered a signal $A = A_1 + \cdots + A_{16}$. The veto signal was the subject of much care and was finally made to yield ratios $(B\bar{A})/B$ between 10^{-5} and 5×10^{-5}. The real event rate was typically two orders of magnitude less than this.

The chambers could be triggered either in the neutral trigger mode, $B\bar{A}$, or in a γ-trigger mode, $B\bar{A}T$. The latter mode made use of the two large sheets of scintillator embedded in the γ-shower region in each of the spark-chamber arrays S_1 and S_2 which gave a signal $T = T_1 + T_2 + T_3 + T_4$. The probability of detection of at least one of the two showers in at least one of the two counters was nearly 100%. When the experiment was triggered in the $B\bar{A}T$ mode one or more of A_1-A_{16} was usually removed from the triggering logic and its state displayed on lights photographed with the chambers. This permitted us to study systematically the accidental suppression of true events by occasional leakage of electromagnetic showers into anticoincidence counters.

The film was scanned for the characteristic "topology" consisting of a pair of electromagnetic showers in one array and a neutron conversion in the other. The latter was required to produce charged secondaries which passed through at least one of the 15-g/cm^2 lead plates. The showers were required to originate within the first five chambers of the array, while the neutron conversion was required to occur after this region. The location of the apparent conversion points of the photon and neutron and the beam-chamber tracks were measured for those events which satisfied the topology criterion. A kinematics reconstruction program adjusted these measured positions such as to minimize χ^2 subject to energy-momentum conservation constraints. No information about the location of the hydrogen target was used in this fitting procedure. The hypothesis that the measured vertices corresponded to an elastic charge exchange and subsequent π^0 decay imposed one constraint on the fitting procedure. The χ^2 distribution of the reconstructed events and the distribution of the computed target vertex positions were consistent with negligible background. The reconstructed events were rejected if their χ^2 exceeded 3.0 or if the computed position of the reaction vertex lay more than 1 in. outside the target. A number of checks such as the calculation of the π^0 opening-angle distribution and neutron vertex-position distribution showed that our sample contained very little background, but these quantities were not used in the selection of events.

The overall detection efficiency of the system (geometric and conversion probability) was computed by means of a Monte Carlo program. The detection efficiency varied smoothly, reaching a maximum of slightly over 20% and always exceeding 10% in the t interval for which we present data. The raw cross section, that is, the counts per unit t interval divided by the efficiency at that value of t, was corrected by a number of t-independent factors. The largest corrections were for (a) events rejected in scanning because of the presence of more than one beam-chamber track; (b) events lost as a result of neutron conversions resulting in charged secondaries of insufficient energy to be observed as such; and (c) valid events lost because of a large χ^2 or other restrictions imposed by the reconstruction

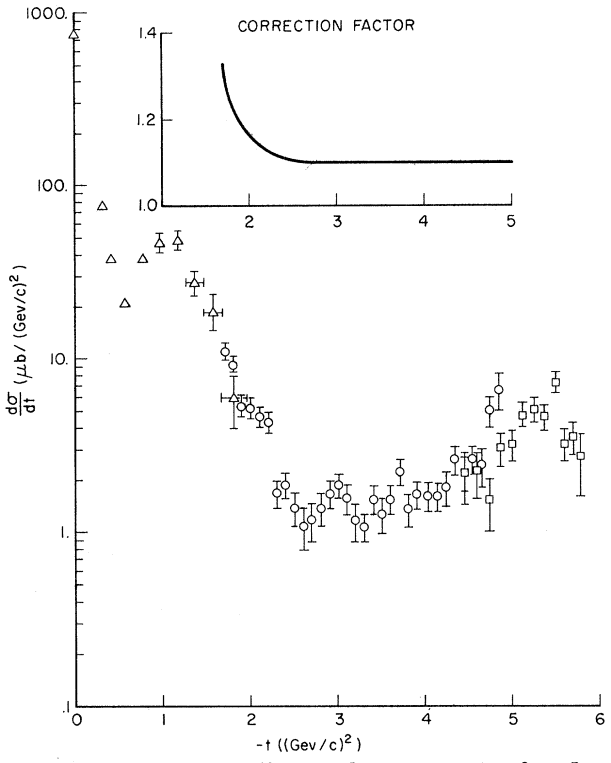

FIG. 2. Measured differential cross section for $\pi^- p \to \pi^0 n$ with an incident π^- momentum of 3.67 GeV/c. Results of this experiment are shown as circles. Triangles are used to plot the data from Ref. 1 at 3.67 GeV/c; squares are used to plot the results of Ref. 2 at 4.0 GeV/c but are plotted at the same u values. The indicated statistical errors in our experiment do not include an overall normalization uncertainty of ±20%. The inset shows the t-dependent corrections made to these data.

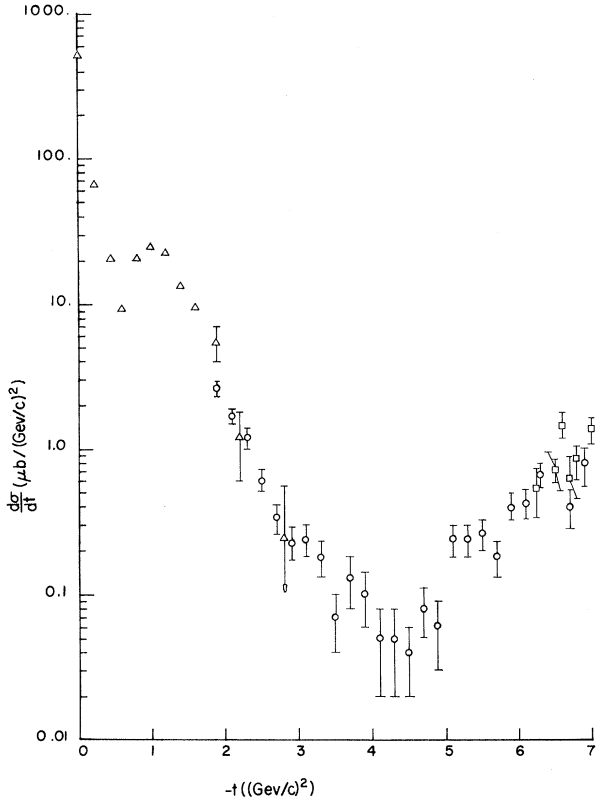

FIG. 3. Measured differential cross section for $\pi^- p \to \pi^0 n$ with an incident π^- momentum of 4.83 GeV/c. Triangles are used to plot the data from Ref. 1 at 4.83 GeV/c; squares are used to plot the results of Ref. 2 at 5.0 GeV/c but are plotted at the same u values. The indicated statistical errors in this experiment do not include an overall normalization error of ±18%.

program. The correction for short neutron secondaries was calculated by extrapolating the observed prong-length distribution to zero length. This correction amounted to a factor of 1.29 at the lower beam momentum and 1.38 at the higher momentum. The overall correction factor amounted to 2.0 ± 0.4 at 3.67 GeV/c and 2.2 ± 0.4 at 4.83 GeV/c. In addition there was a t-dependent correction for low-momentum-transfer events which were vetoed by the leakage of showers into the anticoincidence counters. This correction is shown in Fig. 2 for the 3.67-GeV/c data. It amounted to a factor of 1.5 for the lowest-t bin of the higher-momentum data and was unnecessary for other points.

The results of this experiment are presented in Figs. 2 and 3. They agree well with the data of Sonderegger *et al.*[1] in the forward direction. They also agree with the results of Chase *et al.*[2] in the backward hemisphere when one takes into account that their data were not taken at precisely the same beam momentum as ours. No significant dip is observed in $d\sigma/dt$ in the region of -2.5 to -3.0 (GeV/c)^2. The t resolution in this experiment was computed in the reconstruction program and amounted to 0.1 (GeV/c)^2 and 0.2 (GeV/c)^2 (full width at half-maximum) at the lower and higher beam momentum, respectively. A dip of the shape predicted in Ref. 4 or observed by Rust *et al.*[5] in $\pi^+ p$ elastic scattering at 5 GeV/c would be evident even with a t resolution of 0.4 (GeV/c)^2. Thus we conclude that no dips of this nature exist in the charge-exchange channel for the region studied by this experiment.

The authors wish to thank the staff of the ZGS for their support. We also acknowledge the contributions of F. F. Liu, W. A. Blanpied, W. M. Smith, and A. G. Strelzoff to various aspects of the experiment.

*Work supported by the National Science Foundation

and the U. S. Atomic Energy Commission.

†Now at International Business Machines Corporation, Endicott, N. Y.

[1]P. Sonderegger, J. Kirz, O. Guisan, P. Falk-Vairant, C. Bruneton, P. Borgeaud, A. V. Stirling, C. Caverzasio, J. P. Guillaud, M. Yvert, and B. Amblard, Phys. Lett. 20, 75 (1966).

[2]R. C. Chase, E. Coleman, H. W. J. Courant, E. Marquit, E. W. Petraske, H. F. Romer, and K. Ruddick, Phys. Rev. D 2, 2588 (1970)

[3]H. R. Crouch *et al.*, Phys. Rev. Lett. 21, 849 (1968); M. A. Wahlig and I. Manelli, Phys. Rev. 168, 1515 (1968).

[4]V. Barger and R. J. N. Phillips, Phys. Rev. Lett. 22, 116 (1969).

[5]D. R. Rust, P. N. Kirk, R. A. Lundy, C. E. W. Ward, D. D. Yovanovitch, S. M. Pruss, C. W. Akerlof, K. S. Han, D. I. Meyer, and P. Schmueser, Phys. Rev. Lett. 24, 1361 (1970); B. B. Brabson, R. R. Crittenden, R. M. Heinz, R. C. Kammerud, H. A. Neal, H. W. Paik, and R. A. Sidwell, Phys. Rev. Lett. 25, 553 (1970).

High-Energy Bounds on Scattering Amplitudes and Oscillations in the Diffraction-Peak Region

Virendra Singh
Tata Institute of Fundamental Research, Bombay, India
(Received 30 December 1970)

Rigorous bounds are established on the absorptive part of the scattering amplitude, $A(s,t)$, for t real and within the Lehman-Martin ellipse. This result is used to prove an upper bound on $|d \ln A(s,t)/dt|_{t=0}$, and to show that $A(s,t)$ cannot have a zero in the region $0>t>-4t_0/(\ln s)^2$ for $s\to\infty$ ($\sqrt{t_0}=2m_\pi$ for $\pi\pi$, πN, KN, and NN scattering). No assumption is made about the high-energy behavior of the total cross sections.

The Serpukhov data on particle and antiparticle total cross sections[1] $\sigma_{tot}(s)$ has pointed to a possible failure of the Pomeranchuk theorem.[2] This has led to a reanalysis of the "proofs" and to the derivation of new Pomeranchuk-like theorems.[3] In trying to understand this possible failure in terms of a Regge picture, Finkelstein produced an interesting model involving Regge cuts.[4] This model amplitude turns out to have infinite number of oscillations in the physical region for the scattering. It has been suggested that this feature may be general, provided the particle and antiparticle total cross sections tend to different finite limits.[5]

The purpose of the present investigation is to derive restrictions on high-energy behavior of the scattering amplitudes and, in particular, on the location of the zeros in the physical region, using only general considerations. We make use of only (i) unitarity, (ii) analyticity within the Lehman-Martin ellipse, and (iii) the Jin-Martin upper bound

$$A(s,t_0) \underset{s\to\infty}{<} S^2, \tag{1.1}$$

where $A(s,t)$ is the absorptive part of the scattering amplitude and s and t are, respectively, the squared c.m. energy and momentum transfer variables.[6] The major axis of the Lehman-Martin ellipse is given by $2(1+t_0/2k^2)$, where k is the c.m. momentum. We have $\sqrt{t_0}=2m_\pi$ for $\pi\pi$, πN, πK, KN, and NN scattering. *We shall not make any assumptions about the high-energy behavior of the total cross sections.*

The basic theorem. – The absorptive part of the scattering amplitude, $A(s,t)$, has the partial-wave expansion (for $t_0>t$)

$$A(s,t)=\frac{\sqrt{s}}{k}\sum_{l=0}^{\infty}(2l+1)\,\mathrm{Im}a_l P_l(z), \tag{2.1}$$

where $t=-2k^2(1-z)$ and $\mathrm{Im}a_l \geq 0$ from unitarity. All the results discussed in this paper are derived from the following basic result:

Theorem 1.

$$\max\{J_{M,N}{}^{L}(t,t_0)\,|\,M>L\geq N\} \geq \frac{A(s,t)}{A(s,t_0)} \geq \min\{J_{M,N}{}^{L}(t,t_0)\,|\,M>L\geq N\} \quad (M,N=0,1,2,\cdots), \tag{2.2}$$